Cellulose as an inert matrix for presenting cytokines to target cells: production and properties of a stem cell factor–cellulose-binding domain fusion protein

J. Greg DOHENY*, Eric J. JERVIS*, M. Marta GUARNA*, R. Keith HUMPHRIES†, R. Antony J. WARREN* and Douglas G. KILBURN*[1]

*Department of Microbiology and Immunology, Biotechnology Laboratory, The University of British Columbia, 300-6174 University Boulevard, Vancouver, British Columbia, Canada V6T 1Z3, and †Terry Fox Laboratory, British Columbia Cancer Research Center, British Columbia Cancer Agency, 601 West 10th Avenue, Vancouver, British Columbia, Canada V5Z 1L3

A chimaera of stem cell factor (SCF) and a cellulose-binding domain from the xylanase Cex (CBD_{Cex}) effectively immobilizes SCF on a cellulose surface. The fusion protein retains both the cytokine properties of SCF and the cellulose-binding characteristics of CBD_{Cex}. When adsorbed on cellulose, SCF–CBD_{Cex} is up to 7-fold more potent than soluble SCF–CBD_{Cex} and than native SCF at stimulating the proliferation of factor-dependent cell lines. When cells are incubated with cellulose-bound SCF–CBD_{Cex}, activated receptors and SCF–CBD_{Cex} co-localize on the cellulose matrix. The strong binding of SCF–CBD_{Cex} to the cellulose surface permits the effective and localized stimulation of target cells; this is potentially significant for long-term perfusion culturing of factor-dependent cells. It also permits the direct analysis of the effects of surface-bound cytokines on target cells.

Key words: growth factor, haemopoiesis, steel factor.

INTRODUCTION

Most β-1,4-glycanases are modular proteins comprising two or more independent domains. The binding of many of these enzymes to cellulose is mediated by cellulose-binding domains (CBDs) that serve to increase the effective concentration of enzyme on the substrate [1,2]. CBDs are of interest both for the nature of their interactions with cellulose and for their applications as affinity tags when fused to other proteins [3]. CBDs are classified into families of related amino acid sequences [4]. The bacterium *Cellulomonas fimi* produces a number of enzymes that have CBDs [4]. Those that belong to family IIA of CBDs, especially those from the xylanase Cex (CBD_{Cex}) and the endoglucanase CenA (CBD_{CenA}), are the best understood of the CBDs from *C. fimi* [1,5–10].

CBD_{Cex} adsorbs very rapidly and tightly on crystalline cellulose; the K_a is micromolar [5,8]. Although behaving as though bound irreversibly [5,11,12], CBD_{Cex} is mobile on the surface of sheets of crystalline cellulose [10]. A CBD can be linked to another protein partner with the use of molecular genetic techniques. The binding of a CBD to cellulose is unaffected by its being fused to a heterologous protein [6]. For example, a polypeptide comprising CBD_{CenA} fused at its C-terminus to a short peptide containing the sequence Arg-Gly-Asp [13] promotes the attachment of several lines of mammalian cells to cellulose surfaces and microcarriers [14].

The activation and growth of stem cells *in vivo* involves complex interactions with stromal cells that provide effector proteins. The efficacy of the effectors in stimulating cell proliferation and/or differentiation is modulated by their mode of presentation to the target cells. Cytokines, such as stem cell factor (SCF), occur in both membrane-bound and soluble forms [15]. SCF presented on the surfaces of stromal cells is more effective than soluble SCF in stimulating persistent tyrosine kinase activity of its receptor (c-Kit) on target cells [16] and in increasing the longevity of cultured bone-marrow cells [17].

The properties of CBDs suggested that CBD-cytokine fusion proteins adsorbed on cellulose might be used to present cytokines to target cells. Presenting a fusion protein on particulate cellulose might enhance the activity of the cytokine. The mobility of the CBD on a cellulose surface might allow capping of the receptors on cytokine-sensitive cells after their interaction with a fusion protein adsorbed on a sheet of cellulose. Furthermore, the cytokine could be presented alone, thereby eliminating any effects caused by other molecules on the surfaces of stromal cells.

The particulate cellulose used for such experiments should be highly crystalline, with a relatively uniform particle size, to decrease the size of intraparticulate pores and interparticulate voids present in more amorphous celluloses. Bacterial microcrystalline cellulose (BMCC), produced by *Acetobacter xylinum*, has the desired properties [5]. The cellulose vesicle produced by the alga *Valonia ventricosa* is also highly crystalline; it can be attached to glass surfaces to give a thin, uniform cellulose surface on which CBDs can be adsorbed [10].

Fusion of SCF to CBD_{Cex} was chosen as a suitable vehicle for testing the efficacy of the CBD/cellulose system for presenting a cytokine to a target cell. Here we describe the construction, production and some of the properties of an SCF–CBD_{Cex} fusion protein (see Figure 1). Cellulose carrying adsorbed SCF–CBD_{Cex} is more effective than soluble SCF for presentation to target cells.

EXPERIMENTAL

Production of fusion protein

The gene segment encoding the extracellular domain of murine SCF [18] was fused to the gene segment encoding CBD_{Cex} from

Abbreviations used: BMCC, bacterial microcrystalline cellulose; CBD, cellulose-binding domain; CBD_{CenA}, CBD from the endoglucanase CenA; CBD_{Cex}, CBD from the xylanase Cex; MCAC, metal-chelate-affinity chromatography; SCF, stem cell factor; sH-SFM, supplemented hybridoma serum-free medium.

[1] To whom correspondence should be addressed (e-mail kilburn@unixg.ubc.ca).

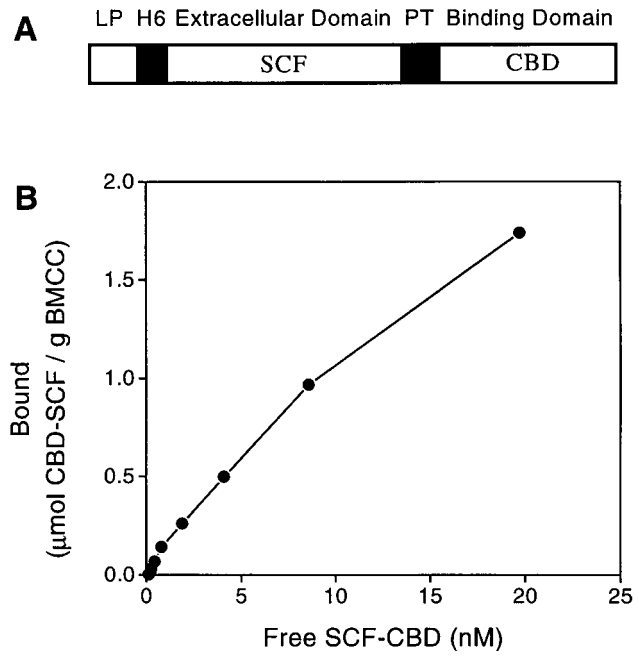

Figure 1 SCF–CBD_{Cex} has a high affinity for cellulose

(**A**) SCF–CBD_{Cex} comprises the CBD and the proline/threonine-rich linker (PT) from the xylanase Cex, the extracellular domain of murine SCF and a hexahistidine affinity tag (H6). The Cex leader peptide (LP), included to facilitate production, is removed in the periplasm of *E. coli*. (**B**) Binding isotherm prepared with fluoresceinated SCF–CBD_{Cex}. SCF–CBD_{Cex} has a K_{app} of 30 μM^{-1} for BMCC. Points are means for triplicate binding reactions.

C. fimi [19]. The mammalian signal sequence was replaced by the Cex signal sequence and the hybrid gene was ligated into the expression vector pTUG AS [20], which had been modified to encode kanamycin resistance (provided by Dr. R. Graham). A polyhistidine affinity tag was inserted after the Cex signal-peptide-processing site to facilitate subsequent purification by metal-chelate-affinity chromatography (MCAC) [21]. The resulting plasmid (pSLF/CBD 1.0) was transformed into *Escherichia coli* JM101 by standard methods. Cultures were grown in 2-litre shake flasks to a D_{600} of 1.0 at 37 °C and 250 rev./min. Isopropyl β-D-thiogalactoside (0.5 mM) was then added and the cultures were shifted to 30 °C and 150 rev./min for a further 8 h. Cells were harvested by centrifugation and the periplasmic fraction was recovered [22]. SCF–CBD_{Cex} was purified from the periplasmic fraction by MCAC. Protein concentrations were determined by measurement of A_{280}. SCF–CBD_{Cex} was labelled with fluorescein isothiocyanate (FITC) in accordance with the manufacturer's recommended protocols (Molecular Probes, Eugene, OR, U.S.A.). The labelled protein was then separated from unbound FITC by MCAC.

Binding isotherms

Isotherms for the binding of SCF–CBD_{Cex} to BMCC were determined as follows. Polypropylene Eppendorf tubes were pretreated with BSA to minimize non-specific adsorption on the tubes. BMCC (40 μg) was mixed with different concentrations of fluoresceinated SCF–CBD_{Cex} in 1 ml of PBS. The tubes were placed on rotating mixers for 3 h at 25 °C in the dark to allow binding. Then the tubes were centrifuged at 10300 ***g*** for 10 min. The supernatants were removed and the concentrations of unbound fluoresceinated SCF–CBD_{Cex} were determined as

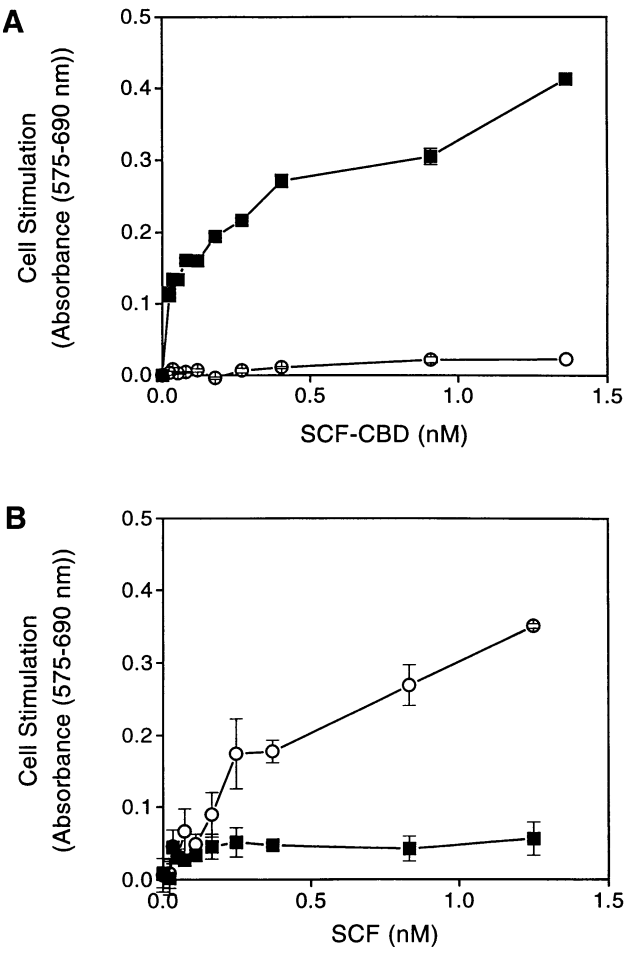

Figure 2 SCF–CBD_{Cex} is active when bound to cellulose

After incubation of SCF–CBD_{Cex} (**A**) or SCF (**B**) with 1 μg/ml BMCC, the cellulose (■) and the liquid phase (○) were separated by centrifugation and tested for stimulatory activity as described in the Experimental section. SCF–CBD_{Cex} activity was associated with cellulose (**A**); SCF activity remained in the liquid phase (**B**).

follows. The supernatants were transferred to tubes pretreated with BSA and containing excess (3.2 mg) Avicel cellulose (FMC International) to adsorb the unbound SCF-CBD_{Cex} in the supernatant. Samples containing known amounts of fluoresceinated SCF–CBD_{Cex} were adsorbed on 3.2 mg of Avicel as standards. Tubes were then placed on a rotating mixer for 24 h at 25 °C in the dark. After binding, the tubes were centrifuged at 10300 ***g*** for 10 min. The Avicel pellets were resuspended in 100 μl of 50 mM phosphate buffer and transferred to wells in a 96-well plate. The fluorescence of fluoresceinated SCF–CBD_{Cex} adsorbed on the Avicel was determined with a 96-well plate fluorimeter (IDEXX, Portland, MA, U.S.A.) at an excitation wavelength of 488 nm and an emission wavelength of 535 nm. Concentrations of fluoresceinated SCF–CBD_{Cex} were determined by reference to the standards. The adsorption isotherm data were analysed by non-linear regression with a Langmuir-type model assuming a single class of binding sites and a total capacity of 4 μmol of FITC-SCF–CBD_{Cex}/g of BMCC [8].

Analysis of stimulatory activities of soluble and immobilized SCF–CBD_{Cex}

Purified SCF–CBD_{Cex}, diluted in 20 μl of serum-free hybridoma medium (Gibco BRL, Grand Island, NY, U.S.A.) supplemented

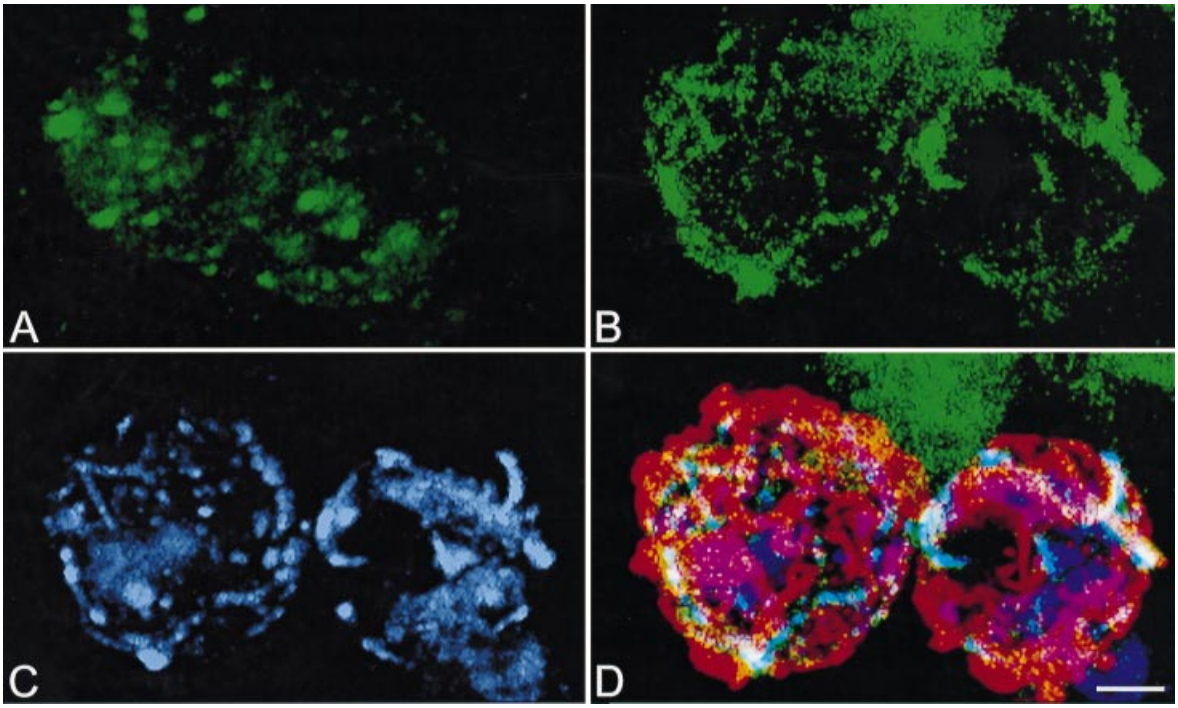

Figure 3 Immunofluorescent laser scanning confocal microscopy of cells stimulated with BMCC-bound SCF–CBD_{Cex}

Cells were incubated with soluble SCF–CBD_{Cex} (**A**) or SCF–CBD_{Cex} adsorbed on BMCC (**B**–**D**). For imaging, cells were labelled with rabbit anti-SCF and biotin-conjugated rat anti-(c-Kit) (SCF receptor) monoclonal antibodies. Secondary labels were FITC-conjugated goat anti-(rabbit IgG) (SCF, green), streptavidin–Cy5 (c-Kit, blue) and phalloidin–Texas Red (actin, red). The morphology of the BMCC fibres is evident in (**B**—**D**). Co-localization of receptor and ligand is confirmed in (**D**). The aquamarine stripes on the cell surface are the result of the interaction of SCF–CBD_{Cex} (green) with c-Kit (blue). The cell cytoskeleton was counterstained with phalloidin–Texas Red to show the cell envelope (red). Scale bar, 5 μm.

with 200 μg/ml human transferrin, 10 μg/ml bovine insulin and 10 mg/ml BSA (sH-SFM), was mixed with 50 μl of a BMCC suspension in the wells of 96-well tissue culture plates (Costar Corp., Cambridge, MA, U.S.A.). After a 12 h incubation at 37 °C in an air/CO_2 (19:1) atmosphere, 100 μl of sH-SFM containing 2×10^4 B6SUtA cells [23] was added to the mixture. After incubation of the cultures for 48 h, cell stimulation was estimated by measuring cell metabolic activity with a standard 3-(4,5-dimethylthiazol-2-yl)-2,5-diphenyl-2*H*-tetrazolium bromide (MTT)-based assay [24]. Murine SCF produced in *E. coli* (R&D Systems, Minneapolis, MN, U.S.A.) was used as control.

Cell proliferation assay

Factor-dependent cell lines were grown to late exponential phase (3 days for MO7e [25] and TF-1 [26] cells; 2 days for B6SUtA cells) in Iscove's modified Dulbecco's medium containing 10 % (v/v) fetal calf serum and supplemented as follows: with 5 % (v/v) murine-spleen-cell-conditioned medium (HemoStim™ M2100; StemCell Technologies, Vancouver, BC, Canada) for B6SutA cells, with 1 ng/ml rhSCF/ml and 5 ng/ml rhIL-3 (StemCell Technologies) for MO7e cells, and with 2 ng/ml rhGM-CSF (StemCell Technologies) for TF-1 cells. The cells were washed three times in sH-SFM, then resuspended in four times the culture volume in sH-SFM. The cell suspension was added to culture wells containing SCF or SCF–CBD_{Cex}, with or without BMCC, as described above. The cultures were incubated for 48 h at 37 °C under air/CO_2 (19:1). Viable cells were determined by Trypan Blue exclusion using a haemocytometer. Dose–response curves were fitted using ORIGIN v. 4.0 (Microcal Software, Northampton, MA, U.S.A.) on the basis of the 24 individual data points from each set. EC_{50} values and standard errors were calculated by using the same software. Non-viable cells constituted less than 5 % of the total cell number in all cases and were not included in the statistical analysis.

Cell imaging with laser scanning confocal microscopy

B6SutA cells were grown as above to late exponential phase, washed twice in sH-SFM and incubated for 6 h at 10^6 cells/ml in sH-SFM without growth factors. Then soluble SCF–CBD_{Cex}, or SCF–CBD_{Cex} adsorbed on BMCC, was added to the cultures. After 20 min, cells were fixed with 4.0 % (w/v) paraformaldehyde, rinsed three times in PBS, then permeabilized by treatment with 0.5 % (v/v) Triton X-100 for 10 min. The fixed cells were blocked for 20 min in 5 % (w/v) BSA, then labelled for 1 h with antibody diluted with 5 % (w/v) BSA. Primary antibodies were as follows: rabbit anti-SCF (polyclonal) and biotin-conjugated rat anti-(murine c-Kit) (monoclonal) (PharMingen, San Diego, CA, U.S.A.). Secondary labels were as follows: FITC-conjugated goat anti-(rabbit Ig) (Sigma, St. Louis, MO, U.S.A.), streptavidin–Cy5 conjugate (Evergreen Labs, Edmonton, Alberta, Canada) and phalloidin–Texas Red conjugate (Molecular Probes, Eugene, OR, U.S.A.).

For analysis of receptor activation, sheets of cellulose were prepared from the cell walls of the marine alga *V. ventricosa*. Sheets dried on glass coverslips were incubated with CBD_{Cex}, SCF or SCF–CBD_{Cex}. After being washed, B6SUtA cells were cultured for 20 h on the cellulose surfaces. For antibody labelling, cells were fixed, permeabilized and blocked as de-

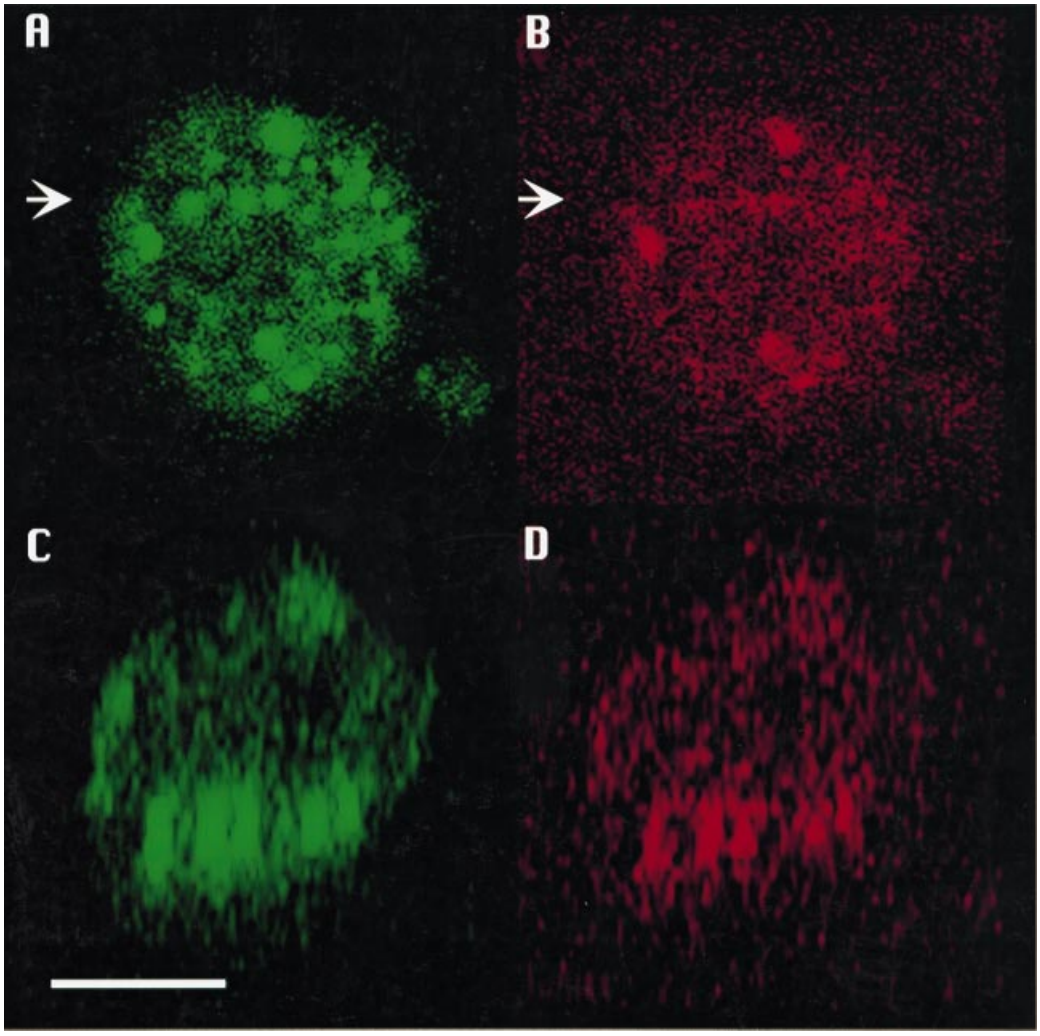

Figure 4 Receptor activation by interaction with immobilized SCF–CBD_{Cex}

B6SUtA cells were incubated on a cellulose sheet to which SCF–CBD_{Cex} was bound. Imaging was performed at the cellulose–cell interface (**A**, **B**) with a depth of focus of approx. 1 μm. Antibody against phosphotyrosine bound to permeabilized cells (**A**) and co-localized in patches with anti-(c-Kit) antibody (**B**). (**C**, **D**) A cross-section (Z-section) perpendicular to the cellulose surface passing through the cell at the plane indicated by the arrows in (**A**) and (**B**). Activation was primarily localized to the cellulose surface (**C**) and co-localized with the anti-receptor antibody (**D**). Scale bar, 10 μm.

scribed above. Primary antibodies were as follows: rabbit anti-CBD_{Cex} (polyclonal), biotin-conjugated rat anti-(mouse c-Kit) (monoclonal) (PharMingen) and mouse anti-phosphotyrosine (monoclonal) (UBI, Lake Placid, NY, U.S.A.). Secondary labels were as follows: FITC-conjugated goat anti-(rabbit Ig), FITC-conjugated goat anti-(mouse Ig) (Sigma) and streptavidin–Texas Red conjugate (Gibco, Grand Island, NY, U.S.A.). Immunofluorescence was imaged with a Bio-Rad MRC600 laser scanning system mounted on a Nikon Axiophot microscope fitted with a $\times 60$ 1.4 numerical aperture objective lens.

RESULTS

SCF–CBD_{Cex} retains the properties of both fusion partners

Purified SCF–CBD_{Cex} retained the properties of each of its constituent domains, binding to cellulose and stimulating the SCF-dependent murine bone marrow cell line B6SUtA (Figures 1 and 2). The K_{app} for the binding of SCF–CBD_{Cex} to BMCC was approx. 30 μM^{-1}, consistent with values reported previously for CBD_{Cex} [5]. In the presence of BMCC, the stimulatory activity of SCF–CBD_{Cex}, but not that of native SCF, was associated with the cellulose (Figure 2), confirming that the binding of SCF–CBD_{Cex} to cellulose was mediated by the CBD.

Formation of SCF–CBD_{Cex}–BMCC–cell complexes

Stimulation with soluble SCF–CBD_{Cex} led to the accumulation of small round patches of SCF–CBD_{Cex} on the surfaces of cells (Figure 3A), whereas stimulation with SCF–CBD_{Cex} adsorbed on BMCC led to elongated irregular patches, which was consistent with the shapes of BMCC fibres (Figure 3B). The cell interacted directly with the fibre presenting SCF–CBD_{Cex}, causing the fibre to conform to the round shape of the cell body. The c-Kit receptor was co-localized with the SCF–CBD_{Cex}–BMCC complex (Figures 3C and 3D). Therefore, when presented on cellulose, SCF–CBD_{Cex} mediated a localized increase in receptor density on the cell membrane at the point of contact between the cell and the fibre.

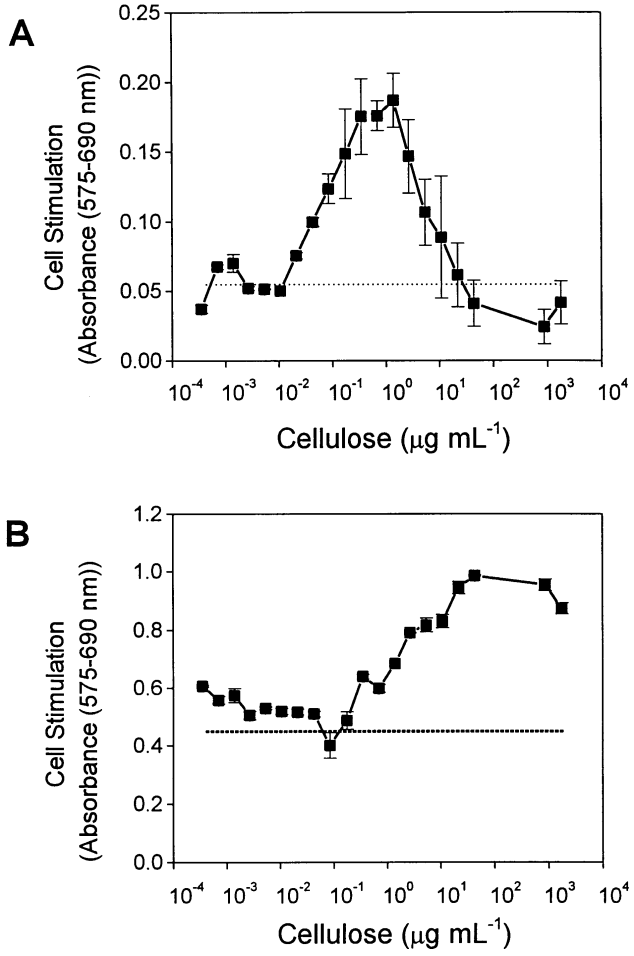

Figure 5 Concentrations of cellulose and SCF–CBD_{Cex} affect the response of B6SUtA cells

The influence of BMCC concentration on the stimulation of B6SUtA cells was tested at SCF–CBD_{Cex} concentrations of 130 pM (**A**) and 1500 pM (**B**). The dotted line represents the activity of SCF–CBD_{Cex} in the absence of cellulose.

Cellulose-bound SCF–CBD_{Cex} causes clustering and polarization of receptors

B6SUtA cells adhered to cellulose surfaces presenting bound SCF–CBD_{Cex} but not to cellulose surfaces pretreated with either SCF or CBD_{Cex} alone. Therefore adhesion required both the CBD_{Cex} and SCF domains of the fusion protein. SCF receptors were concentrated in the areas of contact between B6SutA cells and the cellulose surface. Furthermore, anti-receptor antibodies co-localized with antibodies against phosphorylated tyrosine residues, indicating that the polarized receptors were activated (Figure 4).

Surface density of bound SCF–CBD_{Cex} affects its activity

The binding of SCF–CBD_{Cex} to cellulose increased its stimulatory activity in cultures (Figure 5). The concentrations of both SCF–CBD_{Cex} and the cellulose matrix affected the response of B6SUtA cells in this system. Presumably, at very low concentrations of cellulose the matrix surface area was limiting, whereas at high concentrations of cellulose the surface density of SCF was limiting. Increasing the concentration of SCF–CBD_{Cex} compensated for this effect (Figure 5B), suggesting that there is a surface density of SCF at which activation is optimal. At 0.13 nM SCF–CBD_{Cex}, the concentration of BMCC required for maximum activity was approx. 1 μg/ml (Figure 5A), whereas at 1.5 nM SCF–CBD_{Cex} it was approx. 20 μg/ml (Figure 5B). On the basis of the estimated surface area of the cellulose matrix used in these cultures [5], the critical surface density was approx. 4×10^{10} molecules/cm^2 of cellulose.

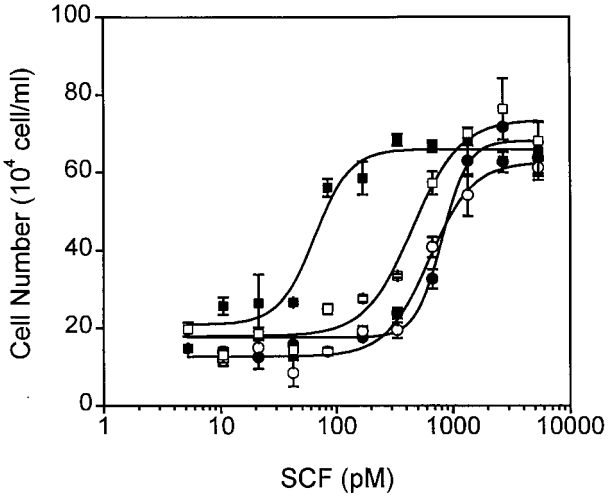

Figure 6 Cellulose enhances the cell proliferation activity of SCF–CBD_{Cex}

A dose–response assay of cell proliferation was performed for SCF–CBD_{Cex} (□,■) and SCF (○,●) in B6SUtA cell cultures with (■,●) or without (□,○) 1 μg/ml BMCC. SCF–CBD_{Cex} was more potent when localized on BMCC.

Enhanced potency of bound SCF–CBD_{Cex} for murine and human SCF-dependent cell lines

Three SCF-dependent cell lines, one murine (B6SutA) and two human (MO7e and TF-1), were used to test the biological activity of SCF–CBD_{Cex} (Figure 6 and Table 1). The EC_{50} values for both SCF and soluble SCF–CBD_{Cex} with MO7E cells were approx. 150 pM, corresponding to approx. 3 ng/ml SCF (which was consistent with the SCF supplier's specifications). The potency of SCF–CBD_{Cex} for all cell lines was enhanced 5–7-fold by adsorption on BMCC (Table 1), whereas the activity of SCF was decreased slightly in the presence of BMCC. Neither cellulose nor CBD_{Cex} exhibited intrinsic growth factor activity (results not shown).

DISCUSSION

SCF–CBD_{Cex} adsorbed on cellulose is an effective vehicle for the presentation of SCF to target cells. The properties of each domain in the SCF–CBD_{Cex} fusion are retained and correct orientation of SCF for receptor binding is facilitated. The density of the cytokine on the cellulose surface seems to be critical for maximal cell stimulation. By using the cellulose–CBD fusion system, both the area of the presenting surface and the density of factor on the surface can be varied. This approach should be applicable to a variety of growth factors and cytokines that trigger activation by receptor clustering. Furthermore, a CBD can be attached to the N-terminus or the C-terminus of a fusion

Table 1 Adsorption of SCF–CBD_{Cex} on cellulose enhances the proliferative effect on murine and human SCF-responsive cell lines

EC_{50} values were calculated from dose–response curves of SCF–CBD_{Cex} and SCF with or without BMCC for B6SutA, MO7e and TF-1 cell lines. Values are means ± S.E.M.

Cell line	SCF–CBD concentration (pM)		SCF concentration (pM)	
	No cellulose	With cellulose	No cellulose	With cellulose
B6SutA	455 ± 58	65 ± 9	629 ± 65	807 ± 75
MO7e	178 ± 42	37 ± 24	124 ± 30	308 ± 33
TF-1	160 ± 22	31 ± 16	349 ± 64	311 ± 53

partner [27,28] or can be located between two domains [29]. This affords significant flexibility of design, allowing the presentation of a single factor in either orientation relative to the cellulose surface or of multiple factors simultaneously.

Previous efforts to immobilize cytokines or growth factors include covalent attachment either directly to surfaces or through linking tethers [30–33]. Covalent attachment might hinder ligand–receptor interaction or prevent receptor dimerization and capping on target cells. Tethering the factor to the surface via an extended linker addresses this problem to some extent but published methods depend on chemical coupling to appropriately positioned reactive groups on target growth factors [32]. If reactive groups are distributed across the surface of the factor or within the active site, it is difficult to ensure correct orientation and full bioactivity when it is immobilized.

Recent advances in bone marrow transplantation and other cell-based graft therapies have intensified the need for technological improvements in primary cell cultivation systems. *In vivo* the activation and growth of progenitor cells involves complex interactions with stroma, which provide an important source of soluble and surface-bound growth factors. Cellulose is an ideal matrix for cytokine immobilization and presentation in cell cultures because it is inert, is available in a wide variety of forms (e.g. membranes, particles and fibres) and is already used in many culture systems (e.g. hollow-fibre reactors). The properties of SCF–CBD_{Cex} suggest that CBD_{Cex} fusions might provide an effective general method for the presentation of factors to cells in culture. Furthermore, this approach facilitates efforts to analyse further the role of growth factor presentation in isolation from other stromal cell effects.

We thank Dr. Roger Graham, Ms. Emily Kwan and Emily Amandoron-Akow for their assistance in protein design and production, and Dr. Ching-An Peng, Dr. Cheryl Helgason, Stephen T.-K. Yip, Soo-Jeet Teh and Dr. Huang-Sia Teh for assistance with cell culturing. This work was supported by grants from the Natural Sciences and Engineering Research Council of Canada, the British Columbia Health Research Foundation and the National Cancer Institute of Canada, with funds from the Canadian Cancer Society and the Terry Fox Run.

REFERENCES

1 Gilkes, N. R., Warren, R. A. J., Miller, Jr., R. C. and Kilburn, D. G. (1988) J. Biol. Chem. **263**, 10401–10407
2 Bolam, D. N., Ciruela, A., McQueen-Mason, S., Simpson, P., Williamson, M. P., Rixon, J. E., Boraston, A., Hazlewood, G. P. and Gilbert, H. J. (1998) Biochem. J. **331**, 775–781
3 Tomme, P., Gilkes, N. R., Guarna, M. M., Haynes, C. A., Hasenwinkle, D., Jervis, E., Johnson, P., McIntosh, L., Warren, R. A. J. and Kilburn, D. G. (1996) in Enzyme Engineering XIII (Dordick, J. S. and Russell, A. J., eds.), Ann. NY Acad. Sci. **79**, 418–424
4 Tomme, P., Warren, R. A. J., Miller, Jr., R. C., Kilburn, D. G. and Gilkes, N. R. (1995) in Enzymatic Degradation of Insoluble Carbohydrates (Saddler, J. N. and Penner, M. H., eds.), Am. Chem. Soc. Symp. Ser. **618**, 142–163
5 Gilkes, N. R., Jervis, E., Henrissat, B., Tekant, B., Miller, Jr., R. C., Warren, R. A. J. and Kilburn, D. G. (1992) J. Biol. Chem. **267**, 6743–6749
6 Ong, E., Gilkes, N. R., Miller, Jr., R. C., Warren, R. A. J. and Kilburn, D. G. (1993) Biotechnol. Bioeng. **42**, 401–409
7 Xu, G.-Y., Ong, E., Gilkes, N. R., Kilburn, D. G., Muhandiram, D. R., Harris-Brandts, M., Carver, J. P., Kay, L. and Harvey, T. S. (1995) Biochemistry **34**, 6993–7009
8 Creagh, A. L., Ong, E., Jervis, E. J., Kilburn, D. G. and Haynes, C. A. (1996) Proc. Natl. Acad. Sci. U.S.A. **93**, 12229–12234
9 Bray, M. R., Johnson, P. E., Gilkes, N. R., McIntosh, L. P., Kilburn, D. G. and Warren, R. A. J. (1996) Protein Sci. **5**, 2311–2318
10 Jervis, E. J., Haynes, C. A. and Kilburn, D. G. (1997) J. Biol. Chem. **272**, 24016–24023
11 Ong, E., Gilkes, N. R., Miller, Jr., R. C., Warren, R. A. J. and Kilburn, D. G. (1991) Enzyme Microb. Technol. **13**, 59–65
12 Tomme, P., Boraston, A., McLean, B., Kormos, J., Creagh, A. L., Sturch, K., Gilkes, N. R., Haynes, C. A., Warren, R. A. J. and Kilburn, D. G. (1998) J. Chromatog. B **715**, 283–296
13 Wierzba, A., Reichl, U., Turner, R. F. B., Warren, R. A. J. and Kilburn, D. G. (1995) Biotechnol. Bioeng. **47**, 147–154
14 Wierzba, A., Reichl, U., Turner, R. F. B., Warren, R. A. J. and Kilburn, D. G. (1995) Biotechnol. Bioeng. **46**, 185–193
15 Broudy, V. C. (1997) Blood **90**, 1345–1364
16 Miyazawa, K., Williams, D. A., Gotoh, A., Nishimaki, J., Broxmeyer, H. E. and Toyama, K. (1995) Blood **85**, 641–649
17 Toksoz, D., Zsebo, K. M., Smith, K. A., Hu, S., Brankow, D., Suggs, S. V., Martin, F. H. and Williams, D. A. (1992) Proc. Natl. Acad. Sci. U.S.A. **89**, 7350–7354
18 Anderson, D. M., Lyman, S.D., Baird, A., Wignall, J. M., Eisenman, J., Raunch, C., March, C. J., Boswell, H. S., Gimpel, S.D., Cosman, D. and Williams, D. E. (1990) Cell **63**, 235–243
19 O'Neill, G., Goh, S. H., Warren, R. A. J., Kilburn, D. G. and Miller, Jr., R. C. (1986) Gene **44**, 325–330
20 Graham, R. W., Greenwood, J. M., Warren, R. A. J., Kilburn, D. G. and Trimbur, D. E. (1995) Gene **158**, 51–54
21 Ausubel, F. M., Brent, R., Kingston, R. E., Moore, D. D., Deidman, J. G., Smith, J. A. and Struhl, K., eds. (1992) Current Protocols in Molecular Biology, Wiley Interscience, New York
22 Nossal, N. G. and Heppel, L. A. (1966) J. Biol. Chem. **241**, 3055–3062
23 Greenberger, J. S., Sakakeeny, M. A., Humphries, R. K., Eaves, C. J. and Eckner, R. J. (1983) Proc. Natl. Acad. Sci. U.S.A. **80**, 2931–2935
24 Denizot, F. and Lang, R. (1986) J. Immunol. Methods **89**, 271–286
25 Avanzi, G. C., Brizzi, M. F., Giannotti, J., Ciarietta, A., Yang, T.-C., Pegoraro, L. and Clark, S. C. (1990) J. Cell. Physiol. **145**, 458–464
26 Kitamura, T., Tange, T., Terasawa, T., Chiba, S., Kuwaki, T., Miyagawa, K., Piao, Y.-F., Miyazono, K., Urabe, A. and Takaku, F. (1989) J. Cell. Physiol. **140**, 323–334
27 Assouline, Z., Shen, H., Kilburn, D. G. and Warren, R. A. J. (1993) Protein Eng. **6**, 787–792
28 Greenwood, J. M., Gilkes, N. R., Miller, R. C., Kilburn, D. G. and Warren, R. A. J. (1994) Biotech. Bioeng. **44**, 1295–1305
29 Tomme, P., Gilkes, N. R., Miller, Jr., R. C., Warren, R. A. J. and Kilburn, D. G. (1993) Protein Eng. **7**, 117–123
30 Cuatrecasas, P. (1969) Proc. Natl. Acad. Sci. U.S.A. **63**, 450–457
31 Ito, Y., Liu, S. Q., Nakabayashi, M. and Imanishi, Y. (1996) Proc. Natl. Acad. Sci. U.S.A. **93**, 3598–3601
32 Kuhl, P. R. and Griffith-Cima, L. G. (1996) Nat. Med. (N.Y.) **2**, 1022–1027
33 Horwitz, J. I., Toner, M., Tompkins, R. G. and Yarmush, M. J. (1993) Molec. Immun. **30**, 1041–1048

Received 14 September 1998/14 December 1998; accepted 18 January 1999